Numerical and experimental characterization of internal heat and mass transfer during convective drying of papaya (*Carica papaya L.)* in a drying air stream

Fouakeu-nanfack Gildas Armel [1*], Kewou Serge[1], Ngouem Felix Junior[1], Tetang Fokone Abraham[1], Edoun Marcel[1], Zeghmati Belkacem[2]

[1] *Applied Energy and Thermal Laboratory, ENSAI-University of Ngaoundere, CAMEROON*
[2] *Laboratory of Mathematics and Physics, University of Perpignan via Domitia, FRANCE*

[*]*Corresponding author E-mail: fouakeunanfack@gmail.com*

Abstract – *This work consisted of simulating convective heat and mass transfers during the drying of papaya in a parallel air stream. The aim of this work was to simultaneously couple the two-dimensional heat and mass transfer equations in the product in order to predict the drying kinetics of the papaya. These papaya slices were arranged on a rack with a length (L) of 30 cm and thickness (E) of 5 mm. The Luikov equations thus established for this model were discretized using the implicit finite difference method and then solved simultaneously using the Matlab 2014 tool. Simulations of papaya drying were performed under the influence of drying air temperature (40, 50, and 60 °C), drying air velocity (0.5, 1 and 1.76 m/s), relative air humidity (20, 40, and 60%), and product thickness (4, 5, and 6 mm). The numerical simulation results allowed the prediction of the temperature and humidity distributions inside the product during the drying process. The predicted data from this model were compared to the experimental data. The results showed agreement between the predicted and experimental data with average relative errors of 5.21% and 4.35% for moisture ratio and product temperature, respectively.*

Keywords: Characterization, Heat and mass transfer, Convective drying, Air stream.

Received: 10/10/2023 – Revised: 23/11/2023 – Accepted: 12/12/2023

I. Introduction

Numerous agricultural items, including the huge numbers of fruits and vegetables that we consume, are not constantly in season. These produce items are a significant source of vitamins and minerals for human nutrition because of their high vitamin and mineral content [1]. The majority of these products are harvested at extremely high humidity levels. It must be sold or consumed fresh within a very short period of time due to the perishable nature of the product which makes it vulnerable to numerous contaminations (molds, bacteria, etc…) [2]. Otherwise, it degrades and loses its suitability for food. Additionally, small-scale farmers who depend on their little plots of land for their livelihood are vulnerable to market changes, particularly during the growing seasons when prices fall to the point that production is in deficit. To get over this obstacle, a number of strategies have been put forth, including greenhouse culture, freezing, and drying. Drying is a quick, secure, and effective way to cut post-harvest loss Drying is an operation whose purpose is to partially or totally eliminate water from a wet body by evaporation [3]. In Sub-Saharan African countries, this technique can extend the shelf life of most food crops in general, and of high moisture content products in particular (moisture content between 60 and 90%), which are highly perishable products. One of the most commonly used methods is convective drying, which consists of sending hot air over the product using static dryers with electrical or solar [4] energy to remove moisture. This drying mode inducing heat and mass transfers remains energy intensive despite many optimization works. he improvement of this drying mode and the quality of the products necessarily require an accurate prediction of the transfer phenomena. With this in mind, [5–9] have done a semi-empirical modeling of the drying of agri-foodstuffs in thin films in order to predict the drying kinetics. Nevertheless, the utilization of these models is restricted due to the uniqueness of each model corresponding to the product type and the specific conditions of the drying experiment. As a result, these models cannot be extrapolated past the scope of the experiment. Theoretical modeling is an additional strategy that entails learning the multiple intricate mechanisms of heat and mass transfers that take place within the product. The complexity of the systems under study frequently results in the simplification of some presumptions. The reduction of the drying equations to be studied to 1D by [10,11], to 2D by [12–14]. Some researchers like [15–17] consider mass transfer as the main phenomenon occurring during product drying. On the other hand, [18-20] instead consider heat transfer as the main phenomenon occurring during the drying of agrifood products. The drying of an agrifood product is described by the coupled heat and mass transfer mechanisms that occur simultaneously within the product. These must be taken into account in the two-dimensional modeling of the drying kinetics. This is one of the interests presented by our work, indeed, very few works in the literature addresses the two-dimensional modeling of coupled and simultaneous heat and mass transfers during the drying of food products.

In this work, a theoretical and experimental study of the convective drying of papaya slices is presented. The temperature and moisture distributions within the slice are predicted using theoretical equations based on the Luikov model. Experimental data are used to validate the theoretical model.

II. Materials and methods

II.1. Plant material

The "Solo 8" papayas of the Caricaceae family, a regional variation from the Littoral Region of Cameroon, were the samples used in this study. These papayas were cleaned, peeled, and chopped along the fibers. Using the caliper, the product was cut into slices that measured 9 cm in length and 5 mm in thickness. The electronic balance was used to estimate the beginning weight of the samples, with an error of 0.01 g.

II.2. Experimental device

The studies were carried out in a 1.2 x 0.2 x 0.2 (m^3) electric parallel airflow drier. It is furnished with three identical racks, each measuring 0.3 x 0.19 (m^2) in size. The racks are placed horizontally inside the dryer and exposed to a parallel air flow, as shown in Figure 1. This experimental tool was created and constructed by [10] in Laboratory of Energetics and Applied Thermal (LETA) of the National School of Agro-Industrial Sciences (ENSAI). When the electric drying air stream is activated, an electric current is drawn via the heating resistors, which causes the Joule effect, which dissipates heat. The temperature of this gadget is controlled by an electric controller called the XSTC-200t that has a Pt100 probe. A rheostat linked in series with the fan controls the air flow of the drying air stream as well. During the tests, the weight of the product was determined using an Adam Nimbus NBL 2602 digital scale (accuracy of reading: 0.01 g), the temperature of the ambient air, drying air, and product was determined using type K thermocouples (accuracy of reading: 0.5 °C), the relative humidity was determined using an Almemo FHAD 46-Cx hygrometer (accuracy of reading: 0.2%), and the velocity of the drying.

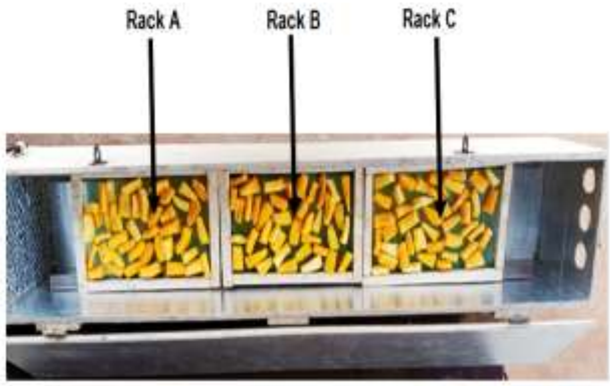

Figure 1. Layout of racks in the dryer

II.3. Physical modeling of papaya drying

The studied system, represented in Figure 1 is composed of a wet product arranged on a rack, having the characteristics of a papaya with a length (L) of 30 cm and a thickness (E) of 5 mm. The vertical sides of the product are considered adiabatic and impermeable to the material. The two upper and lower sides of the product represent the permeable interface, exposed to a hot air flow parallel to the free surface of the product. The drying conditions (velocity V_a, temperature T_a and mass fraction C_{va}) of the hot air are assumed to be constant at the plate inlet. The coordinate system adopted is shown in Figure 2.

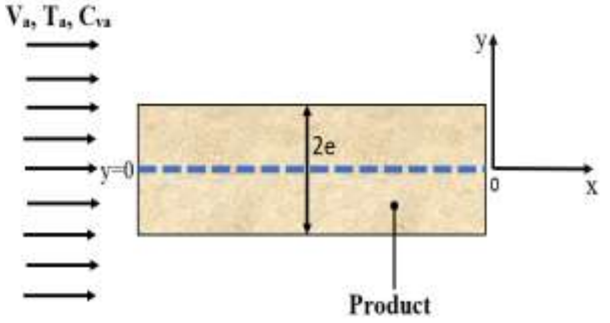

Figure 2 . Representation of the physical model of the papaya

II.4. Hypotheses

To simplify the formulation of the equations, we make the following assumptions [21]:

- The problem is fully symmetric about a median plane;
- The fluid is incompressible and Newtonian;
- The flow regime is turbulent and stationary;
- The deformation of the product during drying is negligible;
- The physical properties of the product and the air are variable;
- The radiative exchanges inside the chamber are negligible;
- The temperature and moisture content are initially uniform in the product.

II.5. Mathematical formulation of transfer equations

Given the simplifying assumptions made above, the convection equations in the product are written as follows [22]:

❖ Mass transfer equation

$$\frac{\partial X_p}{\partial t} = D_{eff}\left(\frac{\partial^2 X_p}{\partial x^2} + \frac{\partial^2 X_p}{\partial y^2}\right) \quad (1)$$

❖ Heat transfer equation

$$\rho_p C_{pp}\frac{\partial T_p}{\partial t} = \lambda_p\left(\frac{\partial^2 T_p}{\partial x^2} + \frac{\partial^2 T_p}{\partial y^2}\right) \quad (2)$$

Where C_{pp} is specific heat of the mass of product (kJ/kg °C); D_{eff} is effective diffusivity coefficient (m^2/s); T_p is temperature of product (°C); X_p is moisture content of the product (kg/kg.db); ρ_p is density of product (kg/m^3) and λ_p is thermal conductivity of product (W/m°C).

II.6. Initial conditions

Initially, we have according to hypothesis (7), a uniform temperature and moisture content. This translates mathematically into [22]:

$$t = 0\begin{cases} X_p(x,y,t) = X_p(x,y,0) = X_{p0} \\ T_p(x,y,t) = T_p(x,y,0) = T_{p0} \end{cases}$$

II.7. Boundary conditions

- Heat transfer

On the surface: (j=N_y)

$$\lambda_p \left.\frac{\partial T_p}{\partial y}\right|_{y=0} = h\left(T_a - T_p\right) + h_m\left(X_p - X_a\right) * L_v \quad (3)$$

In the median plane: (j=1)

$$-\lambda_p\left(\frac{\partial T_p}{\partial x} + \frac{\partial T_p}{\partial y}\right) = 0 \quad (4)$$

- Mass transfer

On the surface: (j=N_y)

$$D_{eff}\left.\frac{\partial X_p}{\partial y}\right|_{y=0} = h_m\left(X_p - X_a\right) \quad (5)$$

In the median plane: (j=1)

$$-D_{eff}\left(\frac{\partial X_p}{\partial x} + \frac{\partial X_p}{\partial y}\right) = 0 \quad (6)$$

Where

$$L = 4.1868*\left(597 - 0.56*T\right) \ (7); \ X_a = \rho_a C_{va} \quad (8)$$

$$C_{va} = 2.1667*10^{-3} * \frac{Hr}{100} * \frac{P_{vs}(T_a)}{T_a} \quad (9)$$

With

$$P_{vs} = Exp\begin{pmatrix} \dfrac{5.8*10^3}{T_a} + 1.391 - 4.864*10^{-2} T_a + 4.176*10^{-5} T_a^2 \\ -1.445*10^{-8} T_a^2 + 6.545*\ln(T_a) \end{pmatrix} \quad (10)$$

Where C_{va} is mass fraction of water vapor in air; Hr is relative humidity (%); h is convective heat transfer coefficient (W/m^2°C); h_m is Convective mass transfer coefficient (m/s); L_v is latent heat of vaporization (kJ/kg) ; P_{vs} is saturation vapor pressure (bar); T_a is temperature of air (°C); X_a is moisture content of air (kg/m^3) and ρ_a is density of air (kg/m^3).

From the dry-base moisture content (X_p), the moisture ratio (MR) and drying rate (V_s) are calculated from the following correlations [23-25].

$$MR = \frac{X_p}{X_{p0}} \quad (11)$$

$$V_s = \frac{dX_p}{dt} = \frac{X_{pt} - X_{pt+dt}}{dt} \quad (12)$$

The heat transfer coefficient (h) and mass transfer coefficient (h_m) in the above equations can be determined from the average Nusselt and Sherwood numbers for laminar or turbulent flow over flat plates as follows [26] :

- Laminar flow

$$Nu = \frac{h * L}{\lambda_a} = 0.664\,\mathrm{Re}^{0.5}\,\mathrm{Pr}^{0.33} \quad (13)$$

$$Sh = \frac{h_m * L}{D_a} = 0.664\,\mathrm{Re}^{0.5}\,Sc^{0.33} \quad (14)$$

- Turbulent flow

$$Nu = \frac{h * L}{\lambda_a} = 0.0592\,\mathrm{Re}^{0.5}\,\mathrm{Pr}^{0.33} \quad (15)$$

$$Sh = \frac{h_m * L}{D_a} = 0.0592\,\mathrm{Re}^{0.8}\,Sc^{0.33} \quad (16)$$

Where D_a is diffusion coefficient of water vapor (m^2/s); L is product length (m); Re is Reynolds number; Sc is Schmidt number; Sh is Sherwood number and λ_a is thermal conductivity of air (W/m°C).

The product used for the simulation is the specified papaya with its thermo-physical properties. The simulation parameters used are listed in Table 1.

Table 1. Simulation parameters

Parameters	Symbols	Units	Values
Air temperature	T_a	°C	40 - 50 - 60
Air velocity	V_a	m/s	0,5-1-1,76
Relative humidity of the air	Hr	%	20-40-60
Initial moisture content of the papaya	X_{p0}	%	82,64
Initial temperature of product	T_{p0}	°C	25

In this work, the effective diffusivity of papaya slices proposed by [10] is:

$$D_{eff} = 8.1717*10^{-8} * Exp\left(-\frac{16.2622}{8.314\left(T_a + 273.15\right)}\right) \quad (17)$$

The thermo-physical properties of air used in this work were those proposed by [11].

The thermo-physical properties of papaya arranged between 10°C and 90°C, proposed by [27] are given by the following expressions:

- Density

$$\rho_p\left(T_a\right)\big|_{10°C-90°C} = 1.03*10^3 - 7.9*10^{-3}T_a - 3.69*10^{-3}T_a^2 \quad (18)$$

- Specific heat

$$C_{pp}\left(T_a\right)\big|_{10°C-90°C} = 3.93*10^3 + 8.66*10^{-2}T_a + 4.53*10^{-3}T_a^2 \quad (19)$$

- Thermal conductivity of the product

$$\lambda_p\left(T_a\right)\big|_{10°C-90°C} = 5.52*10^{-1} + 1.73*10^{-3}T_a - 6.48*10^{-6}T_a^2 \quad (20)$$

The heat and moisture transfer equations given in (1) and (2) under the corresponding initial and boundary conditions were coupled and solved simultaneously using the implicit finite difference method using Matlab 2014 software.

III. Results and discussion

III.1. Validation of the model

To validate the theoretical results obtained in this work, they were compared with the experimental results presented by [27]. The thermo-physical parameters of the model used are given by [27] and the thermo-physical properties of the air are proposed by [28]. The simulation conditions are identical to the experimental conditions of convective drying of papaya.

Figure 3 shows the evolution of the simulated and experimental moisture ratio of papaya. It is observed that there is a very good adequacy between the theoretical and experimental results. The validation of the results is done by calculating the average relative error between experimental and theoretical values from the following relation:

$$E(\%) = \sum_{i=1}^{n} \frac{\left|Y_{exp} - Y_{sim}\right|}{Y_{exp}} * \frac{100}{n} \quad (21)$$

Where Y_{exp} is the experimental data, Y_{sim} the data simulated and n is the number of sightings.

The result shows a mean relative error of 2.92% for the product's moisture ratio. The model is validated when the average relative error is generally lower or equal to 3%. The value presented in this study being clearly in this range, we can, in view of this result conclude that the transfer model used allows for more accurate results.

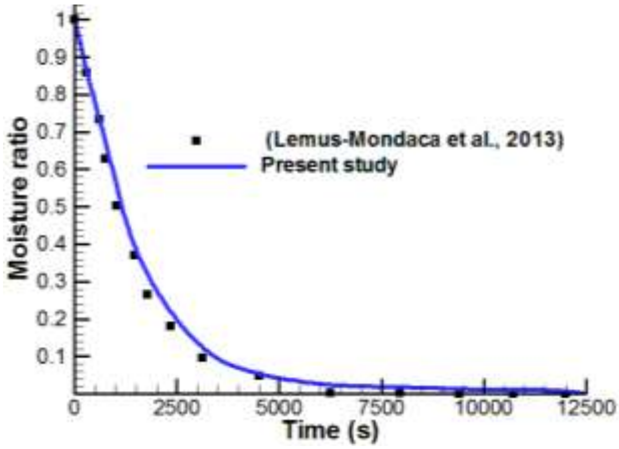

Figure 3 . Comparison of the moisture ratio of the present study simulated with the experimental results of [27] (Ta=60°C ; Va=1,5 m/s ; E=10 mm et L= 30 mm, Hr= 57%)

III.2. Influence of the drying air temperature

Figure 4 shows the evolution of the product temperature as a function of time under the influence of the drying air temperature. On this curve, it is observed that the moisture ratio decreases as a function of time at the different drying temperatures. We notice that during the first 30 minutes, the three curves are merged, indicating the phase of temperature setting of the product. The simulation results show that after 6 hours of drying, the water evaporation power becomes low for the temperature of 60 °C compared to the other temperatures. This behavior is mainly due to the crusting phenomenon, which slows down the evaporation of water on the surface of the product. It is observed on this figure an inverse relationship between the drying time and the air-drying temperature on the moisture ratio.

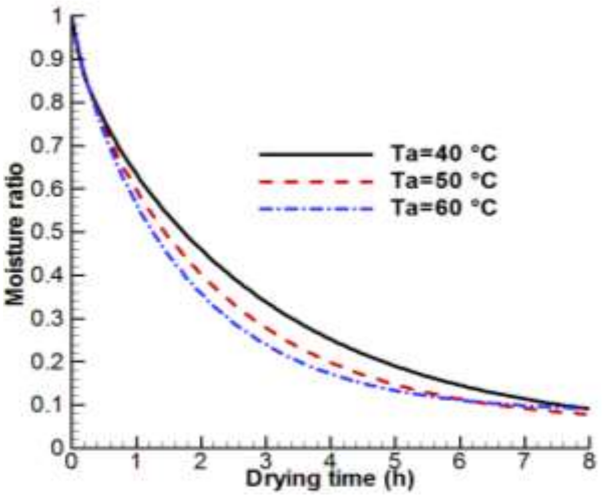

Figure 4 . Evolution of the moisture ratio of the product as a function of time (V_a=1,76m/s; E=0,005m ; Hr=40%)

The Figure 5 shows the evolution of the product temperature as a function of time under the influence of the drying air temperature. The results show that the temperature increases from its initial value of 25 °C and tends towards an asymptotic limit which is the drying air temperature. We also found that the temperature rise time is the same for different values of the drying air temperature. This behavior is only due to the strong dependence of the thickness and the thermal conductivity of the product on the temperature. [29] and [30] present similar evolutions of the bed temperature of agri-food product.

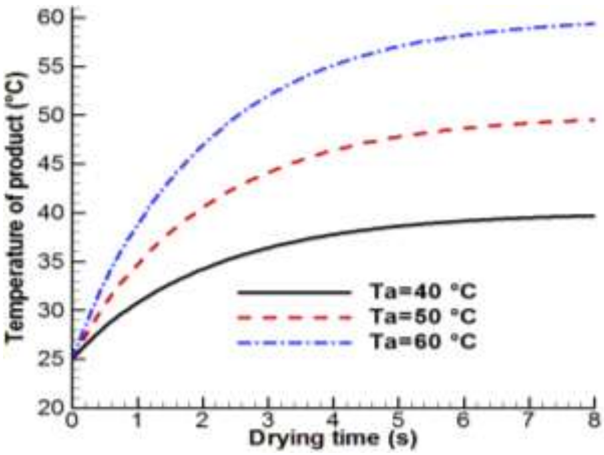

Figure 5 . Evolution of the product temperature as a function of time (V_a=1,76m/s; E=0,005m ; Hr=40%)

We represent in Figure 6 the evolution of the drying rate as a function of time under the influence of the drying air temperature. On these curves, a phase of heating of the product is observed that lasts 10 minutes (the product heats up) followed by another phase of decrease where the movement of water is carried out of the interior towards the surface of the product. Moreover, it is noted that the quantity of evaporated water is more important when the temperature of the drying air is high. But this trend is reversed after 2 hours and 15 minutes of drying. This behavior is due to the phenomenon of crusting which is consistent with the work of [31] on the convective drying of the apple.

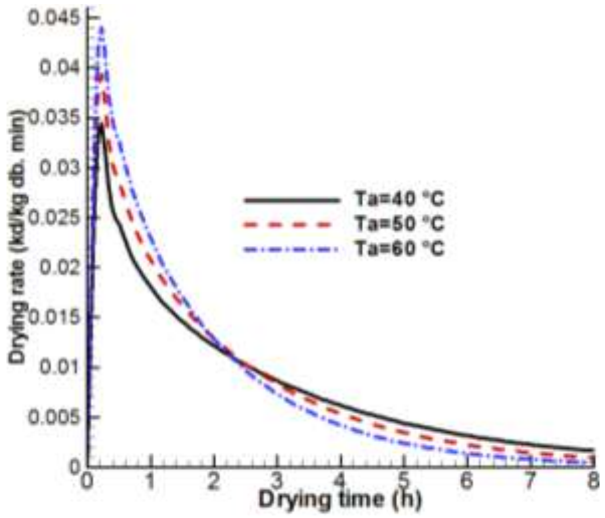

Figure 6 . Evolution of the drying rate as a function of time (V_a=1,76m/s; E=0,005m ; Hr=40%)

III.3. Influence of the drying air velocity

Figure 7 represents the evolution of the moisture ratio as a function of time under the influence of the velocity of the drying air. It is observed on this curve that the moisture ratio decreases as a function of time for the different drying air velocity with very few significant deviations, thus presenting a confusion of the curves. These results showed that the influence of air velocity during the drying of papaya is very insignificant because the internal resistance to moisture transfer is considered preponderant. These results are similar to the work of [32] on vegetables; [33] on hazelnuts, and [34] on pistachios.

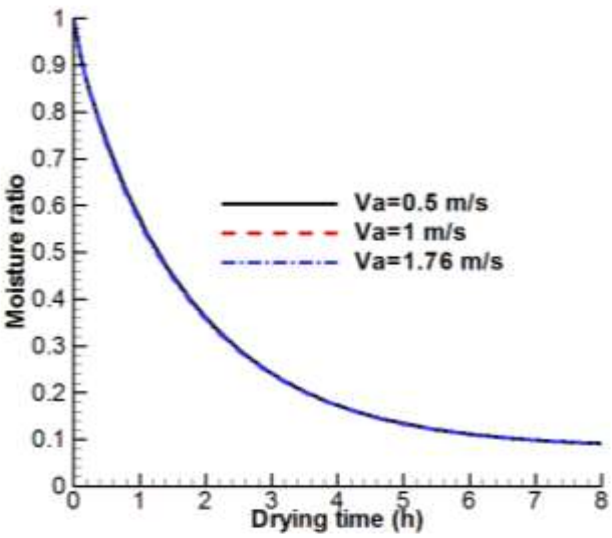

Figure 7 . Evolution of the moisture ratio of the product as a function of time (T_a= 60°C ; E=0,005m ; Hr=40%)

III.4. Influence of the thickness of the product

We represent in Figure 8 the evolution of the moisture ratio as a function of time under the influence of the thickness of the product. We represent in Figure 9 the evolution of the drying rate as a function of time under the influence of the thickness of the product. The results show that after 8 hours of drying, the moisture ratio reach values of 0.0821, 0.0913 and 0.1213 for the values of the product thickness of 4 mm, 5 mm and 6 mm, respectively. It was found that before the thermal equilibrium of the product, the moisture ratio decreases by 4.6% with the increase of one millimeter of product thickness because the path of water diffusion from the inside to the surface of the product is longer. Therefore, it is clear that the decrease in product thickness promotes faster drying of agri-food products which is consistent with the work of [29] where the drying rate also decreases by 4.5% with the increase of one millimeter of product thickness when drying mango.

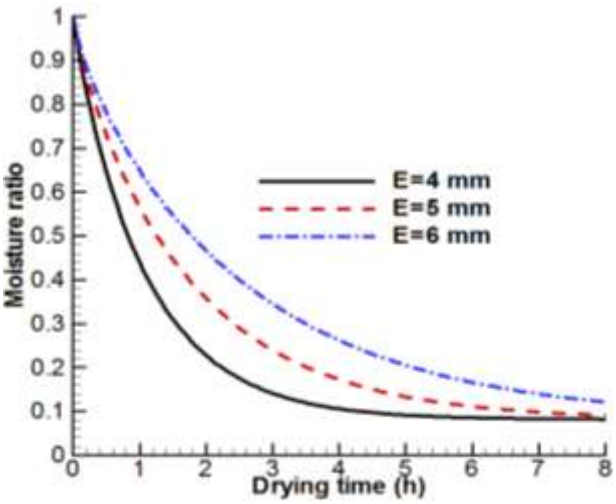

Figure 8 . Evolution of the moisture ratio of the product as a function of time (T_a= 60°C ; V_a=1,76m/s; Hr=40%)

We represent in Figure 9 the evolution of the drying rate as a function of time under the influence of the thickness of the product. For this curve, we observe a phase of heating of the product that lasts 10 minutes (the product heats up) and another phase of decrease where the movement of water is carried out of the interior towards the surface of the product. Moreover, it is observed that the quantity of water evaporated is higher when the thickness of the product is small. But this trend is reversed after 1 hour and 45 minutes of drying; this behavior is due to the phenomenon of crusting. These results are similar to the work of [31] on apples and [35] on papayas.

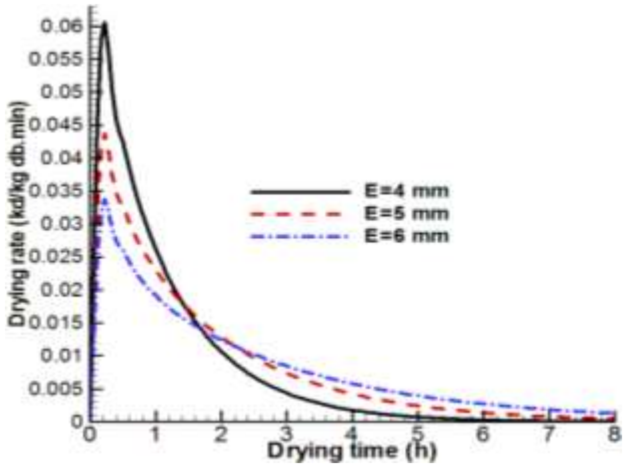

Figure 9 : Evolution of the water content of the product as a function of time (T_a= 60°C ; V_a=1,76m/s ; Hr=40%)

III.5 influence of the humidity of the drying air

Figure 10 shows the evolution of the moisture ratio as a function of time under the influence of the relative humidity of the drying air. The results show that after 8 hours of drying, the values of reduced water content reach 0.0511, 0.0913 and 0.1317 respectively, for the relative humidity values of 20, 40 and 60%. The air humidity plays an important role on the behavior of the drying kinetics of food products. It is found that a decrease in the relative humidity of the air leads to a decrease in the drying time and an acceleration of the drying process. The work of [36] studied in the literature the effect of the relative humidity of the drying air on the values of 25, 40, 55 and 70% during the drying of kiwi.

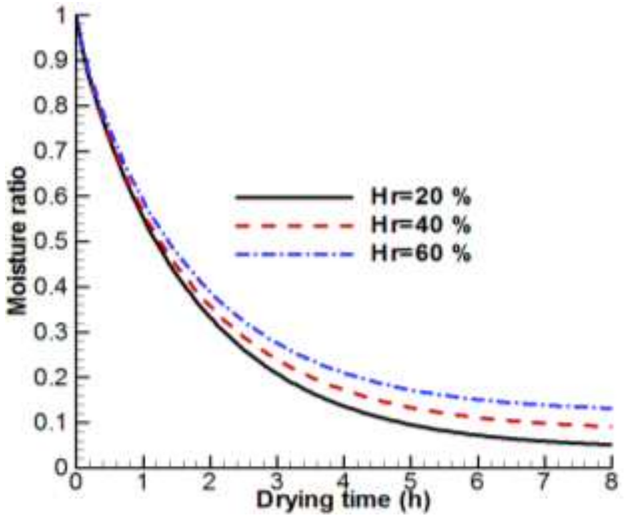

Figure 10 . Evolution of the moisture ratio of the product as a function of time (T_a= 60°C ; V_a=1,76m/s; E=0,005m)

We represent in Figure 11 the evolution of the drying rate as a function of time under the influence of the relative humidity of the drying air. With regard to these curves, we distinguish two phases: the phase of heating up and the phase of slowing down the drying rate. We observe that for these curves, the phase of heating the product lasts 10 minutes (the product heats up). Moreover, it is observed that the drying rate reaches its maximum at 0.04133 kg/kg $_{db.min}$, 0.04181 kg/kg $_{db.min}$ and 0.03781 kg/kg $_{db.min}$ respectively, for humidity rate of 20%, 40% and 60%. This result is in good agreement with the work of [36] regarding thin-film agri-food products.

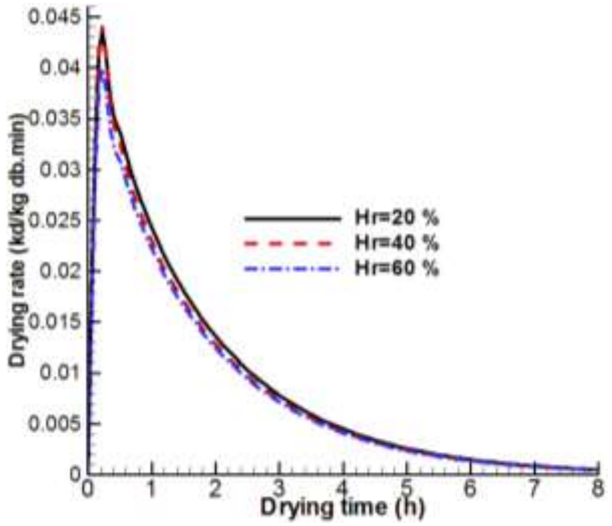

Figure 11 . Evolution of the drying rate as a function of time (T_a= 60°C ; V_a=1,76m/s; E=0,005m)

III.6. Profiles of moisture content distribution in the product

Figure 12 shows the distribution of moisture content in the sample as a function of both space and drying time during air drying at 60 °C. This figure refers to the evolution of moisture content from the surface (2.5 mm) to the center (0 mm) of the sample after 8 hours of drying. We see that the gradients of moisture content from the surface to the center of the sample decrease with increasing drying time, while the moisture content near the center of the sample gradually decreases with drying time. This result is in good agreement with the work of [21] regarding thin-film agri-food products.

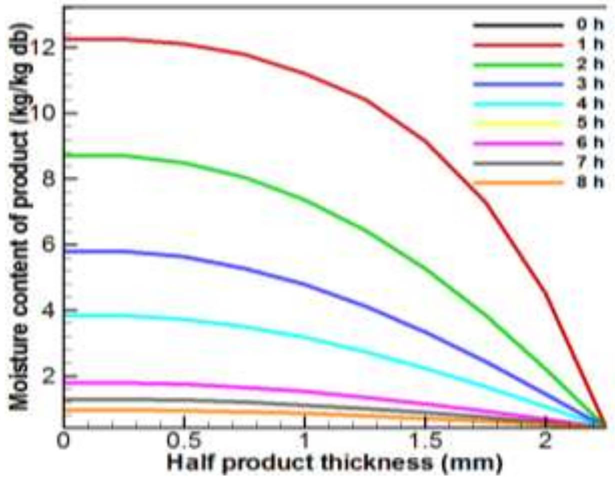

Figure 12 . Evolution of the moisture content as a function of the space produced in for a duration (T_a= 60°C ; V_a=1,76m/s ; E=0,005m ; Hr=40%)

III.7. Comparison of results

Figure 13 shows the comparison of numerical and experimental simulation results of moisture ratio and product temperature as a function of time.

Looking at these curves in Figure 12, we observe that the calculated moisture ratio is higher than the measured temperature. We can see from these figures that the numerical and experimental curves have a similar appearance with appreciable closeness at the beginning and end of the drying process, with the average relative errors being 5.21% and 4.35% for the moisture ratio and the product temperature, respectively. These discrepancies can be explained by the fact that the global transfer coefficients used in these models do not reflect the real behavior of the transfers during drying, hence the need to take into account the parietal boundary layer in the transfer models.

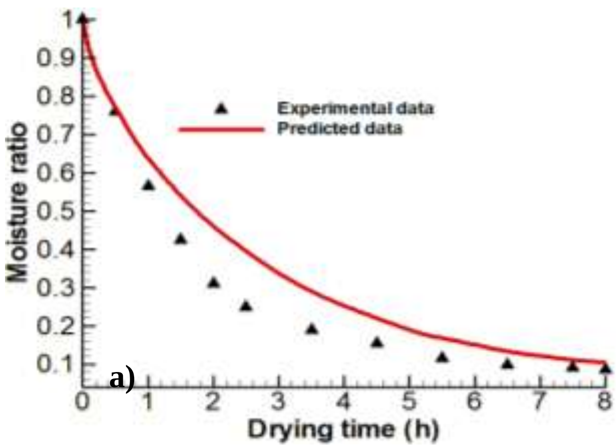

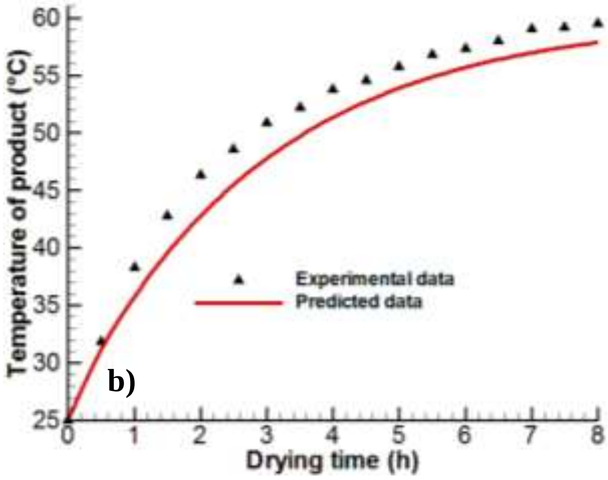

Figure 13: Numerical and experimental simulation of moisture ratio réduite (a) et de la température du produit (b) (Ta=60°C ; V_a=1,76m/s; E=0,005m ; Hr=35%)

IV. Conclusion

This work was concerned with simulating convective heat and mass transfers during the drying of papaya in a parallel air stream. The aim of this work was to simultaneously couple the two-dimensional mass and heat transfer equations in the product in order to predict the drying kinetics of the papaya. The resulting Luikov equations were discretized using the implicit finite difference method and then solved simultaneously using the Matlab 2014 tool. The predicted data from this model were compared to the experimental data. The results showed agreement between the predicted and experimental data, with the average relative errors being 5.21% and 4.35% for the moisture ratio and product temperature, respectively. These gaps can be explained by the fact that the global transfer coefficients used in these models do not reflect the real behavior of the transfers during drying, hence the need to take into account the parietal boundary layer in the transfer models.

Acknowledgement

The authors would like to thank the LETA laboratory of the ENSAI of the University of Ngaoundere for having provided us with the experimental device allowing us to carry out the tests.

Declaration

- The authors declare that they have no known financial or non-financial competing interests in any material discussed in this paper.
- The authors declare that this article has not been published before and is not in the process of being published in any other journal.
- The authors confirmed that the paper was free of plagiarism

References

[1] F. Akter, R. Muhury, A. Sultana, U. K. Deb, ‘‘ A Comprehensive Review of Mathematical Modeling for Drying Processes of Fruits and Vegetables ", International Journal of Food Science, Vol. 2022, pp. 1‑10, 2022, doi: 10.1155/2022/6195257.

[2] A. M. Castro, L. E. Díaz, M. X. Quintanilla-Carvajal, E. Y. Mayorga, F. L. Moreno, ‘‘ Convective drying of feijoa (Acca sellowiana Berg): A study on bioactivity, quality, and drying parameters ", LWT, Vol. 186, pp. 115209, 2023, doi: 10.1016/j.lwt.2023.115209.

[3] A. O. Omolola, A. I. Jideani, P. F. Kapila, ‘‘ Quality properties of fruits as affected by drying operation ", Critical reviews in food science and nutrition, Vol. 57, no 1, pp. 95‑108, 2017, doi: https://doi.org/10.1080/10408398.2013.859563.

[4] J.-P. Nadeau J.-R. Puiggali, ‘‘ Sechage: des processus physiques aux procedes industriels", 1995.

[5] N. G. A. Fouakeu, F. A. Tetang, M. Edoun, A. Kuitche, et B. Zeghmati, ‘‘ A contribution to a numerical characterization of the thermal transfers in a saw tooth solar collector ", International Journal of Thermal Technologies, Vol. 9, no 3, pp. 200‑206, 2019, doi: https://doi.org/10.14741/ijtt/v.9.3.1.

[6] A. S.-S. Stegou–Sagia , A. Fragkou, ‘‘ Thin layer drying modeling of apples and apricots in a solar-assisted drying system", Journal of Thermal Engineering, Vol. 4, no 1, pp. 1680‑1691, 2018, doi: https://doi.org/10.18186/journal-of-thermal-engineering.364909.

[7] A. Stegou-Sagia, D. Fragkou, ‘‘ Influence of drying conditions and mathematical models on the drying curves and the moisture diffusivity of mushrooms ", Journal of Thermal Engineering, Vol. 1, no 4, pp. 235‑244, 2015, doi: https://doi.org/10.18186/jte.65158.

[8] Y. R. Ekani, T. F. Abraham, E. Marcel, K. Alexis, ‘‘ Experimental Study of the Drying Kinetics of Mango (mangifera indica L.) during Airflow Drying Licking Countercurrent", American Journal of Food Science and Technology, Vol. 7, no 4, pp. 127‑132, 2019, doi: 10.12691/ajfst-7-4-4.

[9] A. Kushwah, G. Mk, A. Kumar, P. Singh, ‘‘ Application of ANN and prediction of drying behavior of mushroom drying in side hybrid greenhouse solar dryer: An experimental validation", Journal of Thermal Engineering, Vol. 8, no 2, pp. 221‑234, 2021, doi: 10.14744/jten.2021.0006.

[10] G. A. Fouakeu-nanfack, G. T. N. Wilfred, M. Balbine, E. Marcel, Z. Belkacem, ‘‘ Experimental characterization of convective drying of papaya (Carica papaya L.) to licking airflow", International Journal of Current Engineering and Technology, 2023, doi: https://doi.org/10.14741/ijcet/v.13.1.1.

[11] P. Chen, N. Chen, W. Zhu, D. Wang, M. Jiang, C. Qu, Yu Li; Z. Zou, ‘‘ A Heat and Mass Transfer Model of Peanut Convective Drying Based on a Two-Component Structure", Foods, Vol. 12, no 9, Art. no 9, janv. 2023, doi: 10.3390/foods12091823.

[12] G. Takamte, M. Edoun, L. Monkam, A. Kuitche, R. Kamga, ‘‘ Numerical Simulation of Convective Drying of Mangoes (mangifera Indica L.) Under Variable Thermal Conditions " International Journal of Thermal Technologies, Vol. 3, no 2, pp. 48-52, 2013.

[13] D. A. Tzempelikos, D. Mitrakos, A. P. Vouros, A. V. Bardakas, A. E. Filios, D. P. Margaris, ‘‘ Numerical modeling of heat and mass transfer during convective drying of cylindrical quince slices", Journal of Food Engineering, Vol. 156, pp. 10-21, 2015, doi: https://doi.org/10.1016/j.jfoodeng.2015.01.017.

[14] A. Kaya, O. Aydın, C. Demirtaş, ‘‘ Drying kinetics of red delicious apple", Biosystems Engineering, vol. 96, no 4, pp. 517-524, 2007.

[15] W. P. Da-Silva, C. M. e Silva, et J. P. Gomes, ‘‘ Drying description of cylindrical pieces of bananas in different temperatures using diffusion models", Journal of Food Engineering, vol. 117, no 3, pp. 417-424, 2013, doi: https://doi.org/10.1016/j.jfoodeng.2013.03.030.

[16] J. A. Esfahani, H. Majdi, E. Barati, ‘‘ Analytical two-dimensional analysis of the transport phenomena occurring during convective drying: apple slices", Journal of Food Engineering, Vol. 123, pp. 87-93, 2014, doi: https://doi.org/10.1016/j.jfoodeng.2013.09.019.

[17] L. Lagunez-Rivera, I. I. Ruiz-López, M. A. García-Alvarado, M. A. Salgado-Cervantes, ‘‘ Mathematical simulation of the effective diffusivity of water during drying of papaya", Drying Technology, Vol. 25, no 10, pp. 1633-1638, 2007, doi: https://doi.org/10.1080/07373930701590772.

[18] B. Mocelin, L. Oliveira Jr. Daliomar , P. Daniel Chielle, H. Eduardo Tanabe, A. Daniel Bertuol, M. Schwaab, L. Meili show less., ‘‘ Mathematical modeling of thin layer drying of papaya seeds in a tunnel dryer using particle swarm optimization method", Particulate Science and Technology, Vol. 32, no 2, pp. 123-130, 2014, doi: https://doi.org/10.1080/02726351.2013.839015.

[19] G. L. Dotto, L. Meili, E. H. Tanabe, D. P. Chielle, M. F. P. Moreira, ‘‘ Evaluation of the mass transfer process on thin layer drying of papaya seeds from the perspective of diffusive models", Heat and Mass Transfer, Vol. 54, no 2, pp. 463-471, 2018, doi: https://doi.org/10.1007/s00231-017-2128-y.

[20] R. D. Loss, I. P. Santos, E. P. Muniz, J. R. C. Proveti,

P. S. S. Porto, ‘‘ Finite difference solutions for heat transfer during drying of cubic papaya particles ", Procedia Food Science, Vol. 1, pp. 753-761, 2011.

[21] B. Matuam, N. Gnepie, J. Fotsa, A. Tetang, M. Edoun, E. Alexis Kuitche, ‘‘ Numerical Simulation of Heat and Moisture Transfer in Corrugated Walls Dryer", AE, Vol. 7, no 1, pp. 1-10, 2023, doi: 10.11648/j.ae.20230701.11.

[22] F. J. Ngouem, M. Edoun, L. Monkam, A. Tetang, ‘‘ Simulation of Convective Drying with Shrinkage using the Finite Window Method: Application and Validation", American Scientific Research Journal for Engineering, Technology, and Sciences (ASRJETS), Vol. 78, no 1, pp. 39-49, 2021.

[23] S. Nansereko, J. Muyonga, Y. B. Byaruhanga, ‘‘ Influence of Drying Methods on Jackfruit Drying Behavior and Dried Products Physical Characteristics", International Journal of Food Science, Vol. 2022, p. e8432478, sept. 2022, doi: 10.1155/2022/8432478.

[24] R. Y. Ekani, F. A. Tetang, M. Edoun, A. Kuitche, ‘‘ Airflow Drying Licking Countercurrent of Mango (Mangifera Indica L): Experimental Determination of Drying Parameters", International Journal for Research in Applied Science & Engineering Technology Technology (IJRA), pp. 441-445, https://doi.org/ .22214/ijraset.2022.46052 2022.

[25] M. Edoun, B. Matuam, A. Kuitche, ‘‘ Mathematical modelling of thin layer mangoes (Mangifera indica L.) drying process", International Journal of Current Engineering and Technology, Vol. 4, no 5, pp. 3672-3676, 2014.

[26] R. Golestani, A. Raisi, A. Aroujalian, ‘‘ Mathematical modeling on air drying of apples considering shrinkage and variable diffusion coefficient », Drying Technology, Vol. 31, no 1, pp. 40-51, 2013, doi: https://doi.org/10.1080/07373937.2012.714826.

[27] R. A. Lemus-Mondaca, C. E. Zambra, A. Vega-Gálvez, N. O. Moraga, ‘‘ oupled 3D heat and mass transfer model for numerical analysis of drying process in papaya slices", Journal of Food Engineering, vol. 116, no 1, pp. 109-117, mai 2013, doi: 10.1016/j.jfoodeng.2012.10.050.

[28] Y. Jannot, ‘‘ Transferts thermiques. Ecole des Mines Nancy ». 2012.

[29] L. Villa-Corrales, J. J. Flores-Prieto, J. P. Xamán-Villaseñor, E. García-Hernández, ‘‘ Numerical and experimental analysis of heat and moisture transfer during drying of Ataulfo mango", Journal of food engineering, Vol. 98, no 2, pp. 198-206, 2010, doi: https://doi.org/10.1016/j.jfoodeng.2009.12.026.

[30] H. T. Sabarez, ‘‘ Computational modelling of the transport phenomena occurring during convective drying of prunes », Journal of Food Engineering, Vol. 111, no 2, pp. 279-288, juill. 2012, doi: https://doi.org/10.1016/j.jfoodeng.2012.02.021.

[31] Z. Wang, J. Sun, X. Liao, F. Chen, G. Zhao, J. Wu, X. Hu, ‘‘ Mathematical modeling on hot air drying of thin layer apple pomace", Food Research International, vol. 40, no 1, p. 39‑46, 2007.

[32] M. K. Krokida, V. T. Karathanos, Z. B. Maroulis, D. Marinos-Kouris, ‘‘ Drying kinetics of some vegetables », Journal of Food engineering, Vol. 59, no 4, pp. 391-403, 2003.

[33] E. Tarigan, G. Prateepchaikul, R. Yamsaengsung, A. Sirichote, P. Tekasakul, ‘‘ Drying characteristics of unshelled kernels of candle nuts", Journal of Food Engineering, Vol. 79, no 3, pp. 828-833, 2007.

[34] H. Tavakolipour, ‘‘ Drying kinetics of pistachio nuts (Pistacia vera L.) », World Applied Sciences Journal, vol. 12, no 9, p. 1639‑1646, 2011.

[35] J. A. Pandith, ‘‘ Induction heating assisted foam mat drying of papaya pulp: drying kinetics, drying modeling, and effects on quality attributes", Agricultural Engineering International: CIGR Journal, Vol. 20, no 2, pp. 206-215, 2018, doi: http://orcid.org/0000-0003-2143-3385.

[36] A. Kaya, O. Aydın, I. Dincer, ‘‘ Experimental and numerical investigation of heat and mass transfer during drying of Hayward kiwi fruits (Actinidia Deliciosa Planch) ", Journal of Food Engineering, Vol. 88, nº 3, pp. 323‑330, oct. 2008, Consulté le: 17 juin 2021. [En ligne]. Disponible sur: https://www.sciencedirect.com/science/article/pii/S0260877408000952